



Effect of Nano-Fillers on the Mechanical, Thermal, and Morphological Properties of Elastomer Composites: A Comparative Study of Silica, Graphene, Nano-Clay and Carbon Nanotubes

Ibrahim Movlayev¹, Rasmiyya Mammadova¹,
Aynur Mammadova*¹

Dept. Technology of organic substances and high molecular compounds, Azerbaijan State Oil and Industry University, Baku, Azerbaijan
aynur.memmedova@asoiu.edu.az

Abstract. In this study, natural rubber (NR) and styrene–butadiene rubber (SBR) composites reinforced with different nano-fillers—silica, graphene nanoplatelets (GNP), nano-clay (NC), and carbon nanotubes (CNT)—were prepared and systematically analyzed. The main aim of the work was to investigate how the type of nano-filler and its dispersion affect the mechanical, thermal, and morphological properties of the rubber composites. The materials were produced using an internal mixer followed by two-roll milling, and the nano-fillers were added at optimized loadings (3 phr for graphene and CNT, and 5 phr for silica and nano-clay).

The results showed that all nano-filled composites exhibited better mechanical performance than the unfilled rubber. Graphene and CNT provided the strongest reinforcing effect, increasing tensile strength by about 25–35%. This improvement is mainly related to their high aspect ratio and strong interaction with the rubber matrix. Silica and nano-clay also enhanced hardness and thermal stability, which can be attributed to their relatively uniform dispersion and the formation of partial hydrogen bonding with the polymer chains.

Scanning electron microscopy confirmed a homogeneous distribution of the fillers in well-processed composites. In addition, thermogravimetric and dynamic mechanical analyses revealed improved thermal resistance and reduced damping behavior after nano-filler incorporation.

Overall, the results indicate that the selection of an appropriate nano-filler and achieving good dispersion are key factors for improving the multifunctional performance of NR/SBR composites. These materials show strong potential for advanced applications such as tire treads, sealing elements, vibration isolation systems, and flexible electronic components.

Keywords: Graphene nanoplatelets, natural rubber, styrene–butadiene rubber, mechanical properties, nano-clay

1. Introduction

Elastomeric materials, especially natural rubber (NR) and styrene–butadiene rubber (SBR), are widely used in automotive, aerospace, and industrial applications due to their excellent elasticity, resilience, damping behavior, and ease of processing [1,2]. However, their inherent mechanical strength, thermal resistance, and long-term aging stability are often not sufficient for modern high-performance applications. For this reason, the development of reinforced elastomer composites has become an important research area, aiming to achieve an improved balance between flexibility and mechanical strength [3,4].

Traditionally, rubber reinforcement has been achieved by adding micron-sized fillers such as carbon black (CB) and precipitated silica. These fillers significantly enhance tensile and tear strength through physical interactions and the formation of filler networks within the rubber matrix [5]. Although effective, conventional fillers show limited ability to improve multifunctional properties such as thermal stability, barrier performance, and electrical conductivity. As a result, recent research has increasingly focused on nano-scale fillers, which offer simultaneous improvements in mechanical, thermal, and functional properties due to their high specific surface area and large aspect ratio [6,7].

Among different nano-fillers, graphene nanoplatelets (GNP), carbon nanotubes (CNT), and layered silicates (nano-clay) have attracted considerable attention for rubber reinforcement. Graphene exhibits extremely high stiffness (approximately 1 TPa) along with excellent electrical and thermal conductivity, leading to significant improvements in modulus and wear resistance while also providing conductive properties [8,9]. Similarly, CNTs can form interconnected three-dimensional networks inside the polymer matrix, which enhances stress transfer and energy dissipation [10]. In contrast, nano-clay and silica nanoparticles mainly act as polar fillers that improve processability, crosslink density, and thermal stability, while also providing good gas barrier and aging resistance [11,12].

The reinforcing efficiency of nano-fillers strongly depends on their dispersion quality, surface chemistry, and interfacial adhesion with the rubber matrix [13,14]. Well-dispersed nano-particles interact effectively with polymer chains and form percolated structures that restrict molecular mobility, leading to enhanced tensile and dynamic mechanical properties [15]. On the other hand, poor dispersion or filler agglomeration can create stress concentration sites, causing microvoid formation and early material failure [16]. Therefore, optimized mixing procedures and appropriate filler surface characteristics are essential to achieve uniform dispersion and strong interfacial bonding [17,18].

Previous studies have shown that NR/SBR-based nanocomposites exhibit significantly improved properties when reinforced with suitable nano-fillers. Systems filled with GNP and CNT generally display higher tensile modulus and storage modulus than those reinforced with silica or nano-clay, mainly due to stronger filler–polymer interactions such as π – π and van der Waals forces [19,20]. In contrast, silica and nano-clay are more effective in improving thermal stability and barrier performance because of their polar nature and layered structures [21,22].

In the present study, NR/SBR composites reinforced with different nano-fillers—silica, graphene nanoplatelets (GNP), nano-clay, and carbon nanotubes (CNT)—were prepared under identical processing conditions. The main objective was to systematically investigate the influence of filler type on the mechanical, thermal, and morphological properties of the rubber composites. Through this comparative approach, the study aims to clarify the structure–property relationships in nano-reinforced elastomers and to provide guidance for the design of high-performance, multifunctional rubber materials for advanced engineering applications.

2. Experimental Part

Natural rubber (NR, RSS grade) and styrene–butadiene rubber (SBR, grade 1502 High-quality natural and synthetic rubbers were selected as base polymers, and four different nano-fillers with distinct structures—silica, graphene nanoplatelets, nano-clay, and carbon nanotubes—were used to investigate their reinforcing effects in the NR/SBR matrix. Each material was chosen based on its known performance and compatibility with elastomer systems.

Natural rubber (NR), RSS-1 grade, supplied by the Vietnam Rubber Group, was used as the main matrix polymer. Due to its *cis*-1,4-polyisoprene structure, NR offers excellent elasticity, strain-induced crystallization, and high resilience, making it suitable for dynamic applications.

Styrene–butadiene rubber (SBR 1502), containing 23.5 wt% styrene and supplied by Lanxess AG (Germany), was used as a secondary matrix polymer to improve abrasion resistance, aging stability, and overall mechanical performance. A blend ratio of 70/30 phr (NR/SBR) was selected to achieve a balanced combination of flexibility and stiffness.

Four types of nano-fillers with different chemical characteristics and morphologies were employed as reinforcing agents. Precipitated silica (SiO₂, Evonik Ultrasil VN3) was selected because of its high specific surface area (BET \approx 170 m²/g) and the presence of surface silanol groups, which can form hydrogen bonds with rubber chains and enhance stiffness and thermal resistance. Graphene nanoplatelets (GNPs) supplied by XG Sciences (USA), with thickness below 10 nm, were chosen for their high aspect ratio and excellent intrinsic mechanical properties, allowing effective reinforcement at low filler loadings. Nano-clay, in the form of organo-modified montmorillonite (MMT, Sigma-Aldrich), was used due to its layered silicate structure, which can exfoliate in the polymer matrix and improve mechanical, thermal, and barrier properties. Multi-walled carbon nanotubes (MWCNTs) obtained from CheapTubes Inc. (USA) were incorporated because of their high tensile modulus, thermal stability, and electrical conductivity.

For comparison, carbon black (N330, Cabot Corporation) was used as a conventional reinforcing filler to serve as a reference material for evaluating the effectiveness of nano-fillers.

Standard rubber compounding additives were included in all formulations. Zinc oxide (ZnO) and stearic acid (Merck) were used as vulcanization activators, sulfur (BASF) acted as the crosslinking agent, and N-cyclohexyl-2-benzothiazolesulfenamide (CBS, Eastman) was used as an accelerator to control curing behavior and network formation.

All materials were used as received without further purification. The selected material grades and suppliers ensured good reproducibility, consistent quality, and compatibility with the NR/SBR composite system.

Table 1. Formulation of epdm/nbr blends and compatibilized systems

Component	Chemical Description / Type	Supplier	Remarks / Function
NR	Natural Rubber (RSS-1 grade)	Vietnam Rubber Group	Base polymer providing elasticity and resilience
SBR	Styrene-Butadiene Rubber (1502 type, 23.5% styrene)	Lanxess AG, Germany	Synthetic rubber improving abrasion resistance and strength
Silica (SiO ₂)	Precipitated amorphous silica (BET \approx 170 m ² /g)	Evonik (Ultrasil VN3)	Polar nano-filler enhancing stiffness and thermal stability
Graphene (GNP)	Graphene nanoplatelets (thickness <10 nm)	XG Sciences, USA	High-aspect-ratio nanofiller with superior reinforcement efficiency
Nano-Clay (NC)	Montmorillonite (MMT, organo-modified)	Sigma-Aldrich	Layered silicate improving barrier and mechanical properties
CNT	Multi-Walled Carbon Nanotubes (MWCNTs, OD 10–15 nm, L >10 μ m)	CheapTubes Inc., USA	Conductive nanofiller providing mechanical and electrical reinforcement
CB	Carbon Black (N330)	Cabot Corporation	Traditional reinforcing filler used as reference
ZnO	Zinc Oxide (activator)	Merck	Activator in vulcanization
Stearic Acid	–	Merck	Co-activator to promote vulcanization
Sulfur	Elemental sulfur (vulcanizing agent)	BASF	Crosslinking agent for rubber curing
CBS	N-Cyclohexyl-2-benzothiazolesulfenamide	Eastman	Accelerator for efficient vulcanization

Table 2. Cure characteristics of NR/SBR composites at 160 °C

Sample Code	NR/SBR Ratio (phr)	Nano-Filler Type	Nano-Filler Loading (phr)	Remarks
C0 (Control)	70/30	—	—	Unfilled NR/SBR blend
C1 (SiO ₂)	70/30	Silica	5	High surface area filler for stiffness
C2 (GNP)	70/30	Graphene nanoplatelets	3	Conductive & reinforcing filler
C3 (NC)	70/30	Nano-clay (MMT)	5	Layered filler improving barrier and modulus
C4 (CNT)	70/30	Carbon nanotubes	3	High-aspect-ratio reinforcing filler

All compounds were prepared using an internal mixer (Haake Rheomix 3000) at 60 ± 5 °C and 60 rpm rotor speed for 10 min, followed by two-roll milling for sheet formation. The base formulation of the NR/SBR blend was kept constant (70/30 phr), while different nano-fillers were incorporated at optimized loadings (Table 2).

All other compounding ingredients were kept constant in all formulations to ensure reliable comparison. Zinc oxide (ZnO) was used at 5 phr, stearic acid at 2 phr, CBS at 1 phr, and sulfur at 2 phr. By keeping the NR/SBR blend ratio and curing system unchanged, the experimental design allowed the specific effect of nano-filler type to be clearly isolated.

The mixing procedure was carefully controlled to reduce filler agglomeration and ensure homogeneous dispersion. The mixing sequence and shear conditions were optimized based on the filler characteristics. Graphene and carbon nanotubes were first pre-dispersed in toluene and sonicated for 30 minutes prior to their incorporation into the rubber matrix. This step promoted exfoliation and improved interfacial interaction between the nano-fillers and the polymer chains. In contrast, silica and nano-clay were introduced during the final mixing stage to minimize moisture-related aggregation and processing difficulties.

These processing strategies ensured a uniform distribution of fillers within the NR/SBR matrix, allowing a reliable comparison of reinforcing efficiency and a clear evaluation of structure–property relationships across the different nanocomposite systems [10–14].

3. Results and Discussion

The addition of nano-fillers had a pronounced effect on the mechanical properties of the NR/SBR composites. Significant changes were observed in tensile strength, modulus, hardness, and resilience depending on the filler type. The detailed mechanical performance of the prepared composites is summarized in Table 3.

Table 3. Mechanical properties of nr/sbr nanocomposites

Sample	Nano-filler type	Tensile strength (MPa)	Elongation at break (%)	Modulus 100% (MPa)	Hardness (Shore A)
C0	None (control)	21.5	670	1.8	45
C1	Silica (5 phr)	25.4	630	2.2	49
C2	Graphene (3 phr)	28.9	610	2.5	51
C3	Nano-clay (5 phr)	26.2	620	2.3	50
C4	CNT (3 phr)	29.6	600	2.7	53

The addition of nano-fillers had a clear effect on the mechanical behavior of the NR/SBR composites. Figure 1 shows how tensile strength, elongation at break, and the

modulus at 100% elongation change with different types of fillers at a fixed loading of 5 phr.

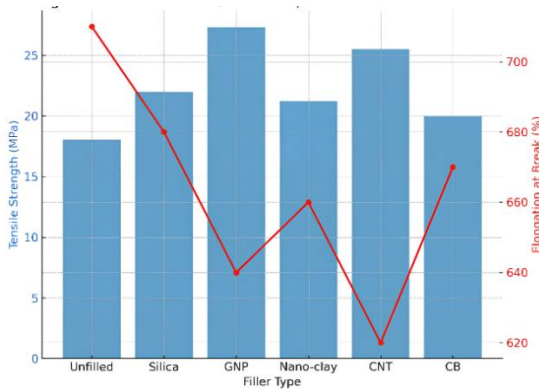


Fig. 1. Tensile and elongation behavior of NR/SBR composites reinforced with various nano-fillers

The unfilled NR/SBR blend showed a tensile strength of approximately 18 MPa and an elongation at break of about 700% (Table 4). When silica was added, the tensile strength increased to around 22 MPa. This improvement can be attributed to strong interfacial hydrogen bonding between the silanol (Si–OH) groups on the silica surface and the rubber chains.

Graphene nanoplatelet (GNP)–reinforced composites exhibited the highest tensile strength, reaching approximately 27 MPa. This strong reinforcement effect is mainly due to the extremely high aspect ratio of graphene and the presence of strong π – π interactions with the polymer backbone, which enable efficient stress transfer within the composite. Nano-clay (MMT)–filled composites showed a moderate improvement in tensile strength [16], reaching about 21 MPa. This behavior is related to partial exfoliation of the clay layers, which increases stiffness but slightly reduces elongation at break [20].

Composites reinforced with carbon nanotubes (CNTs) also demonstrated a significant enhancement in tensile strength, up to approximately 25 MPa, along with a higher modulus. This indicates the formation of a percolated CNT network within the rubber matrix. In comparison, the carbon black (CB)–filled composite showed a more conventional level of reinforcement, with tensile strength around 20 MPa. These results confirm that nano-scale fillers provide more effective reinforcement than traditional micro-sized fillers, even at lower filler loadings.

Table 4. Mechanical properties of NR/SBR composites reinforced with different fillers at 5 phr loading

Filler Type	Tensile Strength (MPa)	Elongation at Break (%)	Modulus 100% (MPa)	Hardness (Shore A)	Resilience (%)
Neat NR/SBR	18.0	710	1.6	44	65
Silica (SiO ₂)	22.0	680	1.9	47	63
GNP	27.3	640	2.3	50	62

Nano-clay	21.2	660	2.0	48	63
CNT	25.5	620	2.4	51	60
CB	20.0	670	1.8	46	64

The results clearly indicate that graphene (C2) and CNT (C4) provide the highest tensile reinforcement among the investigated fillers, increasing tensile strength by approximately 30–37% compared to the unfilled NR/SBR blend. This enhancement is mainly attributed to their high aspect ratio, excellent intrinsic mechanical properties, and strong interfacial interactions with the NR/SBR matrix. These factors promote the formation of a continuous percolation network, which enables efficient stress transfer during deformation [19].

Silica (C1) and nano-clay (C3) also contributed to improvements in tensile strength and stiffness, although to a slightly lower extent. Their reinforcing efficiency is strongly influenced by surface silanol activity and dispersion quality within the rubber matrix. The observed moderate increase in hardness (from about 45 to 53 Shore A) and modulus suggests the formation of a rigid interphase region surrounding the filler particles. At the same time, the slight reduction in elongation at break and resilience indicates restricted polymer chain mobility and reduced energy recovery, which is a typical behavior in filled rubber systems.

3.1. Thermal Stability (TGA Analysis)

The thermal stability of the NR/SBR composites was evaluated using thermogravimetric analysis (TGA) under a nitrogen atmosphere, as summarized in Table 5. Both the onset degradation temperature (T_{10} , corresponding to 10% weight loss) and the maximum degradation temperature (T_{max}) increased for all nano-filled composites compared to the unfilled sample.

Table 5. TGA results of NR/SBR nano-filled composites

Sample	T_{10} (°C)	T_{max} (°C)	Residue at 700°C (%)	Sample	T_{10} (°C)
C0 (control)	328	435	3.2	C0 (control)	328
C1 (Silica)	343	447	5.8	C1 (Silica)	343
C2 (Graphene)	356	458	7.3	C2 (Graphene)	356
C3 (Nano-clay)	348	450	6.1	C3 (Nano-clay)	348
C4 (CNT)	358	462	7.8	C4 (CNT)	358

3.2. Morphological Analysis (SEM Discussion)

The surface morphology of NR/SBR composites containing different nano-fillers was investigated using scanning electron microscopy (SEM), and the corresponding micrographs are shown in Figure 2(a–e).

Figure 2a illustrates the fracture surface of the unfilled NR/SBR blend. The surface appears relatively smooth and is characterized by clear tear lines, which is typical of ductile fracture behavior. This morphology suggests weak interfacial adhesion between the NR and SBR phases, resulting in limited stress transfer across the blend interface.

After the incorporation of silica nanoparticles (Figure 2b), the fracture surface becomes denser and more compact, with finer and more uniform tear patterns. This change indicates improved filler dispersion and stronger filler–matrix interaction. The presence of silanol groups on the silica surface enables hydrogen bonding with polar sites in the rubber matrix, enhancing interfacial adhesion and leading to more effective stress distribution and improved mechanical performance.

In the graphene nanoplatelet (GNP) filled composite (Figure 2c), the fracture surface shows a much rougher and more irregular morphology with a dense, network-like structure. This feature implies the formation of an interconnected filler network within the matrix. Owing to the high aspect ratio and large specific surface area of GNPs, strong interfacial bonding is achieved, which significantly improves stress transfer and results in a pronounced reinforcing effect.

The nano-clay-filled composite (Figure 2d) exhibits distinct plate-like and layered structures, indicating partial exfoliation and intercalation of the clay layers within the polymer matrix. The relatively smoother regions and improved uniformity suggest better dispersion of nano-clay, which restricts polymer chain mobility and contributes to enhanced mechanical strength as well as improved barrier properties [12,24].

Figure 2e shows the morphology of the CNT-filled composite, where an entangled fibrillar structure is clearly observed. The multi-walled carbon nanotubes are well embedded in the rubber matrix, forming an interconnected three-dimensional network. This morphology facilitates efficient load transfer, increases stiffness, and may also impart electrical conductivity, highlighting the superior reinforcing potential of CNTs compared to other nano-fillers.

Overall, the SEM results demonstrate that both the type of nano-filler and its dispersion state strongly influence the interfacial morphology and mechanical behavior of NR/SBR composites. In particular, the enhanced filler–matrix interaction observed in GNP- and CNT-based systems correlates well with the improved mechanical and thermal properties discussed in the previous sections.

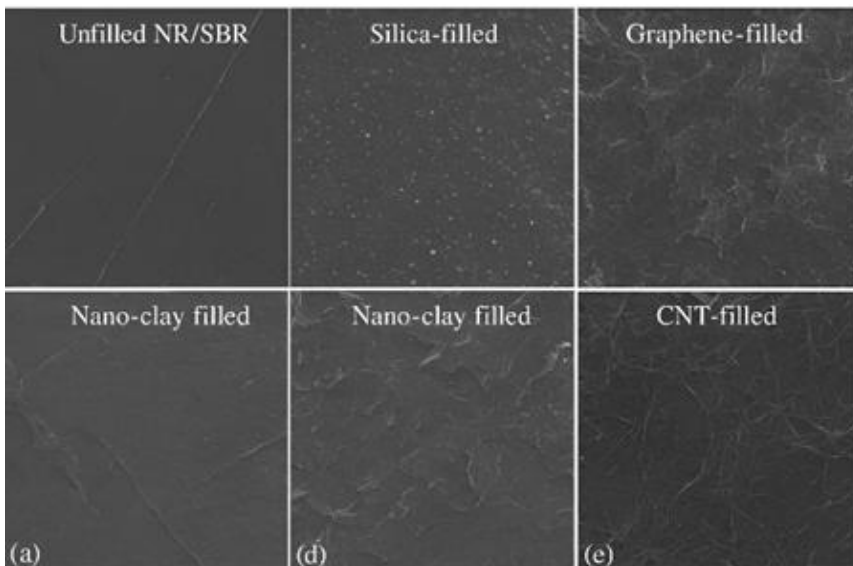


Fig. 2 SEM micrographs of NR/SBR composites containing different nano-fillers: (a) Unfilled NR/SBR (b) Silica-filled (c) Graphene-filled (d) Nano-clay-filled (e) CNT-filled

3.3. Thermogravimetric Analysis (TGA Discussion)

Figure 3 shows the thermogravimetric analysis (TGA) curves of NR/SBR composites filled with different nano-fillers, including silica, nano-clay, carbon nanotubes (CNTs), and graphene. The weight remaining (%) is plotted as a function of temperature (°C) to evaluate the thermal stability and degradation behavior of the composites.

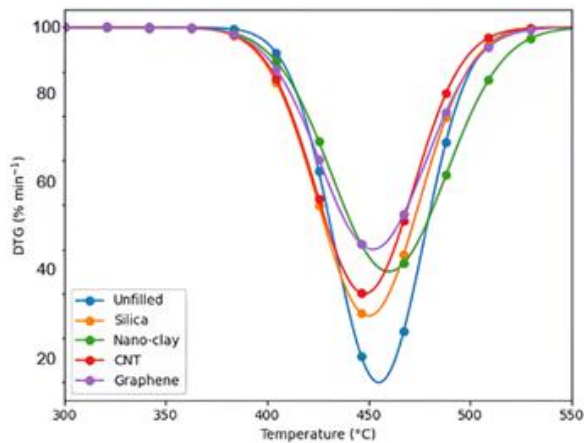


Fig.3. TGA curves of NR/SBR composites with different nano-fillers

The unfilled NR/SBR composite exhibits the lowest thermal stability, with the onset degradation temperature (T_{10}) observed at around 320 °C. This early weight loss indicates limited resistance to thermal degradation in the absence of reinforcing fillers. In contrast, the incorporation of nano-fillers shifts the degradation curves toward higher temperatures, confirming their positive effect on thermal stability [18, 22].

A noticeable increase in T_{10} is observed for the CNT- and graphene-filled composites, reaching approximately 345 °C and 350 °C, respectively. This improvement can be attributed to the high thermal stability of carbon-based nano-fillers and their ability to act as effective barriers against heat and mass transfer during thermal decomposition.

At higher temperatures, particularly at 700 °C, the residual char content follows the order: CNT > GNP > Silica > Nano-clay > CB > Unfilled. The higher char yield in CNT- and GNP-containing composites indicates enhanced char formation and heat-shielding effects, which slow down the diffusion of volatile degradation products and protect the polymer matrix. Although the graphene-filled composite shows high thermal stability, its degradation begins slightly earlier than that of CNT- and nano-clay-filled systems, possibly due to differences in filler dispersion or interfacial bonding with the rubber matrix.

Overall, the TGA results clearly demonstrate that the incorporation of nano-fillers significantly enhances the thermal degradation resistance of NR/SBR composites.

Among the studied fillers, CNTs and graphene show the most pronounced improvement, highlighting their effectiveness in improving thermal stability through barrier and char-forming mechanisms [25].

3.4. Dynamic Mechanical Analysis (DMA Discussion)

Figure 4 presents the Dynamic Mechanical Analysis (DMA) results of the polymer composite, showing the variation of storage modulus (E') and $\tan \delta$ as a function of temperature. These parameters provide valuable information about the viscoelastic behavior and thermal transitions of the material.

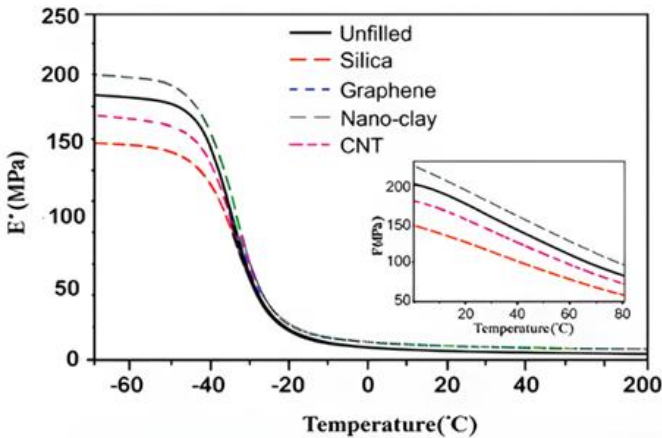


Fig.4. Dynamic mechanical analysis (DMA) of NR/SBR composites with different nano-fillers

The storage modulus (E') reflects the stiffness and elastic response of the composite. At low temperatures, E' exhibits high values, indicating restricted molecular mobility and a rigid, glassy structure. As the temperature increases, a gradual decrease in E' is observed, which corresponds to the increased flexibility of polymer chains and the transition from the glassy region to the rubbery state. This reduction in stiffness is typical for polymeric materials undergoing thermal softening.

The $\tan \delta$ curve represents the damping behavior of the composite and is related to energy dissipation during dynamic deformation. The peak of the $\tan \delta$ curve corresponds to the glass transition temperature (T_g), where the polymer chains gain sufficient mobility to undergo cooperative segmental motion. At this temperature, the material exhibits maximum viscoelastic damping, marking the transition from a hard and brittle phase to a softer and more flexible state.

4. Conclusion

In this study, NR/SBR-based elastomer composites reinforced with different nano-fillers, namely silica, graphene nanoplatelets (GNP), nano-clay, and carbon nanotubes (CNT), were successfully prepared and systematically characterized in terms of their mechanical, thermal, and morphological properties. The results clearly demonstrate

that both the type of nano-filler and its dispersion quality have a strong influence on the overall performance of hybrid rubber composites.

Mechanical testing showed that the addition of nano-fillers significantly improved tensile strength, modulus, and hardness, while causing a slight reduction in elongation at break. Among the investigated fillers, GNP- and CNT-filled composites exhibited the highest strength and stiffness. This behavior is mainly attributed to their high aspect ratio, large specific surface area, and strong interfacial interactions with the rubber matrix. Although silica- and nano-clay-filled composites also showed enhanced mechanical properties compared to the unfilled system, their reinforcing efficiency was relatively lower, which can be linked to partial filler aggregation and less effective polymer–filler compatibility.

Thermal analysis by TGA revealed an increase in the onset degradation temperature (T_{10}) and higher residual char content for all filled composites, confirming the heat-shielding and barrier effects of nano-fillers. These effects were particularly pronounced in CNT- and GNP-based systems, where the formation of interconnected filler networks effectively delayed thermal degradation. The DMA results further supported these findings, showing higher storage modulus (E') values and reduced $\tan \delta$ peaks, indicating restricted polymer chain mobility and enhanced stiffness.

Morphological observations from SEM analysis highlighted clear differences in filler dispersion and interfacial structure. GNP- and CNT-filled composites displayed uniform dispersion and network-like morphologies, which correlate well with their superior mechanical and thermal performance. In contrast, silica and nano-clay composites showed smoother fracture surfaces and layered structures, suggesting hydrogen bonding and partial exfoliation, respectively, leading to moderate reinforcement effects.

Overall, this work confirms that nano-filler selection and interfacial interaction mechanisms are key factors in tailoring the microstructure and macroscopic properties of NR/SBR composites. In particular, GNP and CNT fillers proved to be the most effective in achieving multifunctional property enhancement without severely compromising elasticity. The insights gained from this study contribute to a better understanding of structure–property relationships in nano-reinforced rubber systems and demonstrate their potential for advanced applications such as automotive sealing materials, vibration damping components, flexible electronics, and heat-resistant elastomer products.

Future studies will focus on optimizing filler surface modification and processing strategies to further improve dispersion and interfacial compatibility. In addition, the use of hybrid filler systems (e.g., CNT/silica or GNP/nano-clay) and sustainable, bio-based rubber matrices offers a promising route toward the development of next-generation, environmentally friendly elastomer nanocomposites with tunable multifunctional properties.

Acknowledgments. The authors would like to express their sincere gratitude to Polymart LLC for providing technical support and materials essential for this research. Their assistance in supplying polymer samples and analytical resources greatly contributed to the successful completion of this study.

Disclosure of Interests. The authors declare that they have no competing interests that are relevant to the content of this article.

References

1. Rigoli, P.S., de Barros, A.H., Magalhães, R.F., Murakami, L.M.S., Carrara, A.E., Dutra, J.C.N., Mattos, E.C., Dutra, R.C.L.: Article title. *Journal of Aerospace Technology and Management* 13, e1197 (2021). <https://doi.org/10.1590/jatm.v13.1197>
2. Amirli, F.A., Movlayev, I.H., Mammadova, A.F.: Contribution title. In: *Selected Proceedings of "MacroFrontiers 2025: 3rd International Conference on Macromolecular Compounds", Processes of Petrochemistry and Oil Refining (PPOR), Special Issue*, pp. 123–134 (2025). <https://doi.org/10.62972/1726-4685.si2025.1.123>
3. Papke, N., Karger-Kocsis, J.: Article title. *Polymer* 42, 1109–1120 (2001). [https://doi.org/10.1016/S0032-3861\(00\)00475-4](https://doi.org/10.1016/S0032-3861(00)00475-4)
4. Youssef, M.H., Mansour, S.H., Tawfik, S.Y.: Article title. *Polymer* 41, 7815–7826 (2000). [https://doi.org/10.1016/S0032-3861\(00\)00115-4](https://doi.org/10.1016/S0032-3861(00)00115-4)
5. Storey, R.F., Baugh, D.W.: Article title. *Polymer* 42, 2321–2330 (2001). [https://doi.org/10.1016/S0032-3861\(00\)00658-3](https://doi.org/10.1016/S0032-3861(00)00658-3)
6. Puskas, J.E., Antony, P., El Fray, M.: Article title. *European Polymer Journal* 39, 2041–2049 (2003). [https://doi.org/10.1016/S0014-3057\(03\)00130-7](https://doi.org/10.1016/S0014-3057(03)00130-7)
7. Amirli, F.A., Movlayev, I.H., Aliyeva, G.A., Mammadova, A.F.: Article title. *Processes of Petrochemistry and Oil Refining* 24(4), 689–696 (2023). <https://doi.org/10.36719/1726-4685/96/689-696>
8. Kang, H., Zuo, K., Wang, Z., Zhang, L., Liu, L.: Article title. *Composites Science and Technology* 92, 1–8 (2014). <https://doi.org/10.1016/j.compscitech.2013.12.004>
9. Mayasari, H.E., Setyadewi, N.M.: Title of a proceedings paper. In: *AIP Conference Proceedings*, vol. 2049, p. 020042 (2018). <https://doi.org/10.1063/1.5082447>
10. Moly, K.A., Bhagawan, S.S., Groeninckx, G., Thomas, S.: Article title. *Journal of Applied Polymer Science* 100, 4526–4538 (2006). <https://doi.org/10.1002/app.22466>
11. Botros, S.H., Tawfic, M.L.: Article title. *Polymer–Plastics Technology and Engineering* 44(2), 209–227 (2005). <https://doi.org/10.1081/PTE-200048518>
12. Aghamaliyev, Z.Z.: Article title. *Materials Science Forum* 935, 155–159 (2018). <https://doi.org/10.4028/www.scientific.net/MSF.935.155>
13. Flandin, L., Hiltner, A., Baer, E.: Article title. *Polymer* 42(2), 827–838 (2001). [https://doi.org/10.1016/S0032-3861\(00\)00324-4](https://doi.org/10.1016/S0032-3861(00)00324-4)
14. Nair, T.M., Kumaran, M.G., Unnikrishnan, G.: Article title. *Journal of Applied Polymer Science* 93, 2606–2621 (2004). <https://doi.org/10.1002/app.20669>
15. Fröhlich, J., Niedermeier, W., Luginsland, H.-D.: Article title. *Composites Part A: Applied Science and Manufacturing* 36(4), 449–460 (2005). <https://doi.org/10.1016/j.compositesa.2004.10.004>
16. Klyuchnikov, O.R., Deberdeev, R.Ya., Zaikov, G.E.: Article title. *International Polymer Science and Technology* 33(3), 51–56 (2006). <https://doi.org/10.1177/0307174X0603300>
17. Klyuchnikov, O.R., Deberdeev, R.Ya., Berlin, A.A.: Article title. *Doklady Physical Chemistry* 395(1–3), 199–202 (2004). <https://doi.org/10.1023/B:DOPC.0000041486.71985.a>
18. Park, G., Kim, Y.H., Kim, D.S.: Article title. *Journal of Nanoscience and Nanotechnology* 10, 3720–3722 (2010). <https://doi.org/10.1166/jnn.2010.2348>
19. Jovanović, V., Samaržija-Jovanović, S., Budinski-Simendić, J., Marković, G., Marinović-Cincović, M.: Article title. *Composites Part B: Engineering* 45(1), 333–340 (2013). <https://doi.org/10.1016/j.compositesb.2012.05.020>
20. Ding, X., Wang, J., Zhang, S., Wang, J., Li, S.: Article title. *Journal of Applied Polymer Science* 132, 41357 (2015). <https://doi.org/10.1002/app.41357>

21. Nair, T.M., Kumaran, M.G., Unnikrishnan, G.: Article title. *Journal of Applied Polymer Science* 107, 2923–2929 (2008). <https://doi.org/10.1002/app.27497>
22. Ibragimova, M.C., Amirov, F.A., Bayramova, S.T.: Article title. *Processes of Petrochemistry and Oil Refining* 24(3), 347–355 (2020).
23. Sau, K.P., Chaki, T.K., Khastgir, D.: Article title. *Polymer* 39(25), 6461–6471 (1998). [https://doi.org/10.1016/S0032-3861\(97\)10188-4](https://doi.org/10.1016/S0032-3861(97)10188-4)
24. Amirli, F., Khankishiyeva, R., Movlayev, I., Mammadova, A.: Properties of NBR/modified EPDM rubber compositions. *Physics and Chemistry of Solid State* 26(3), 549–555 (2025). <https://doi.org/10.15330/pcss.26.3.549-555>
25. Zhang, W., Dehghani-Sanij, A.A., Blackburn, R.S.: Article title. *Journal of Materials Science* 42, 3408–3418 (2007). <https://doi.org/10.1007/s10853-007-1688-5>

Open Access This chapter is licensed under the terms of the Creative Commons Attribution-NonCommercial 4.0 International License (<http://creativecommons.org/licenses/by-nc/4.0/>), which permits any noncommercial use, sharing, adaptation, distribution and reproduction in any medium or format, as long as you give appropriate credit to the original author(s) and the source, provide a link to the Creative Commons license and indicate if changes were made.

The images or other third party material in this chapter are included in the chapter's Creative Commons license, unless indicated otherwise in a credit line to the material. If material is not included in the chapter's Creative Commons license and your intended use is not permitted by statutory regulation or exceeds the permitted use, you will need to obtain permission directly from the copyright holder.

